

BAR-DRIVEN EVOLUTION AND 2D SPECTROSCOPY OF BULGES

M. Bureau¹, E. Athanassoula², A. Chung³ and G. Aronica⁴

¹*Hubble Fellow, Columbia Astrophysics Laboratory, 550 West 120th Street, 1027 Pupin Hall, MC 5247, New York, NY 10027, U.S.A.,*

²*Observatoire de Marseille, 2 place Le Verrier, F-13248 Marseille Cedex 4, France,*

³*Department of Astronomy, Columbia University, 550 West 120th Street, 1411 Pupin Hall, MC 5246, New York, NY 10027, U.S.A.,*

⁴*Astronomisches Institut, Ruhr-Universität Bochum, D-44780 Bochum, Germany*

Abstract

A multi-faceted approach is described to constrain the importance of bar-driven evolution in disk galaxies, with a special emphasis on bulge formation. N-body simulations of bars are compared to the stellar kinematics and near-infrared morphology of 30 edge-on spirals, most with a boxy bulge. The N-body simulations allow to construct stellar kinematic bar diagnostics for edge-on systems and to quantify the expected vertical structure of bars. Long-slit spectra of the sample galaxies show characteristic double-hump rotation curves, dispersion profiles with secondary peaks and/or flat maxima, and correlated h_3 and V profiles, indicating that most of them indeed harbor edge-on bars. The stellar kinematics also suggests the presence of cold, quasi-axisymmetric central stellar disks. The ionized-gas distribution and kinematics further suggests that those disks formed through bar-driven gaseous inflow and subsequent star formation, which are absent in our simulations. Minimally affected by dust and dominated by Population II stars, K -band imaging of the same galaxies spectacularly highlights radial variations of the bars' scaleheights, as expected from vertical disk instabilities. The light profiles also vary radially in shape but never approach a classic deVaucouleurs law. Filtering of the images further isolates the specific orbit families at the origin of the boxy structure, which can be directly related to periodic orbit calculations in generic 3D barred potentials. Bars are thus shown to contribute substantially to the formation of both large-scale triaxial bulges and embedded central disks. Relevant results from the SAURON survey of the stellar/ionized-gas kinematics and stellar populations of spheroids are also briefly described. Specific examples supporting the above view are used to illustrate the potential of coupling stellar kinematics and linestrengths (age and metallicity), here specifically to unravel the dynamical evolution and related chemical enrichment history of bars and bulges.

Keywords: galaxies: bulges – galaxies: evolution – galaxies: kinematics and dynamics – galaxies: photometry – galaxies: spiral – galaxies: structure

1. Introduction

Conventional wisdom states that the bulges of spiral galaxies are analogous to low-luminosity elliptical galaxies residing at the centers of disks (Davies et al. 1983), and thus probably formed through rapid collapse or merging. There is however mounting evidence against significant merger growth in many bulges and numerous studies argue for the importance of slower (i.e. secular) processes (e.g. Kormendy 1993; Andredakis, Peletier, & Balcells 1995). Given the rapid decrease of the merger and star formation rates since $z \approx 1$, secular evolution mechanisms have probably been non-negligible for some time already, and their relative importance will only increase with time. Most works emphasize the potentially crucial role of bars and other asymmetries in disks (e.g. Friedli et al. 1996; Erwin & Sparke 2002). Theoretical models often involve the growth of a central mass through bar-driven inflow and recurring bar destruction and formation (e.g. Pfenniger & Norman 1990; Friedli & Benz 1993). The efficiency of bar dissolution mechanisms remains however uncertain and bar re-formation requires substantial external gas accretion over the lifetime of a galaxy (e.g. Bournaud & Combes 2002; Shen & Sellwood 2004). In this paper, we thus focus on slow processes which can occur in isolation.

Beside bar formation, which is well-studied and documented, N-body simulations of cold disks systematically show that, soon after their formation, bars should thicken and settle with an increased vertical velocity dispersion, appearing boxy or peanut-shaped (B/PS) when viewed edge-on (e.g. Combes & Sanders 1981; Combes et al. 1990). The large but constant fraction of B/PS bulges across the Hubble sequence ($\approx 45\%$) supports both the importance of this mechanism for real galaxies and its association with bars (e.g. Lütticke, Dettmar, & Pohlen 2000). Although bars are not readily identifiable in edge-on systems and other mechanisms can give rise to axisymmetric B/PS bulges (e.g. Binney & Petrou 1985; Rowley 1988), the particular gaseous kinematics of B/PS bulges further supports the view that they are simply thick bars viewed edge-on (e.g. Kuijken & Merrifield 1995; Merrifield & Kuijken 1999; Athanassoula & Bureau 1999; Bureau & Freeman 1999). Considering that, if proven true, this link would argue that at least 50% of all bulges formed through bar-driven processes, it is crucial to extend those tests to earlier type galaxies, where one might naively think that merging is more important.

In this paper, we thus present generic N-body simulations of bar-unstable disks developing a B/PS bulge (§ 2), and positively compare them to the stellar kinematics (§ 3) and K -band morphology (§ 4) of a sample of 30 spiral galaxies, most with a B/PS bulge. We also present SAURON integral-field observations of a few B/PS bulges which show not only the kinematic and structural signatures of bars, but also rather homogeneous stellar populations, as expected (§ 5). We conclude by supporting the importance of bar-driven evolution (§ 6).

2. N-Body Simulations of Bars

We have run a large number of standard N-body simulations of bar-unstable disks and discuss below a few generic results. Figure 1 contrasts our results for a typical strongly barred case viewed edge-on (at late times) from various viewing angles. The initial conditions consist of a cold luminous exponential disk with constant Q and a live spherical dark halo (see Athanassoula 2003 for more details). No luminous spheroidal component was initially included in the simulations. The prominent thick central component, which would normally be identified with a bulge both morphologically and from the major-axis surface brightness profiles, is thus composed entirely of disk material. It has acquired a large vertical extent through disk vertical instabilities and, as expected, appears round when seen end-on, boxy-shaped at intermediate viewing angles, and peanut-shaped when seen side-on (e.g. Combes et al. 1990).

Based on a large number of similar simulations and Gauss-Hermite fits (van der Marel & Franx 1993), edge-on barred disks typically show the following kinematic signatures along their major-axis (Bureau & Athanassoula 2004): 1) a major-axis light profile with a quasi-exponential central peak and a plateau at moderate radii (Freeman Type II profile); 2) a “double-hump” rotation curve; 3) a rather flat central velocity dispersion peak with a plateau at moderate radii and, occasionally, a local central minimum and secondary peak; 4) an $h_3 - V$ correlation over the projected bar length. h_4 is rather featureless and is in any case hard to measure observationally, so we do not discuss it further. Those kinematic features are all spatially correlated and can be understood from the orbital structure of barred disks. They therefore provide a reliable and practical tool to identify bars in edge-on disks. Contrary to popular belief, so-called “figure-of-eight” position-velocity diagrams (Kuijken & Merrifield 1995; Merrifield & Kuijken 1999) do not occur in the stellar kinematics, as expected for realistic orbital configurations. However, while they are not uniquely related to triaxiality, line-of-sight velocity distributions with a high velocity tail (i.e. an $h_3 - V$ correlation) do appear to be particularly useful tracers of bars. All the characteristic kinematic features identified grow in strength as the bar evolves and do not change significantly for small departures from edge-on. Most can provide useful measurements of the bar length.

3. Stellar Kinematics of Boxy Bulges

As shown in Chung & Bureau (2004), we have obtained similar long-slit stellar kinematics along the major-axis of the 30 edge-on spirals from the sample of Bureau & Freeman (1999), most of which have a B/PS bulge. Comparing those profiles with the N-body bar diagnostics (§ 2), we find bar signatures in 80% of the galaxies, including the SOs. The diagnostics thus appear robust and support the formation of most B/PS bulges through bar thickening.

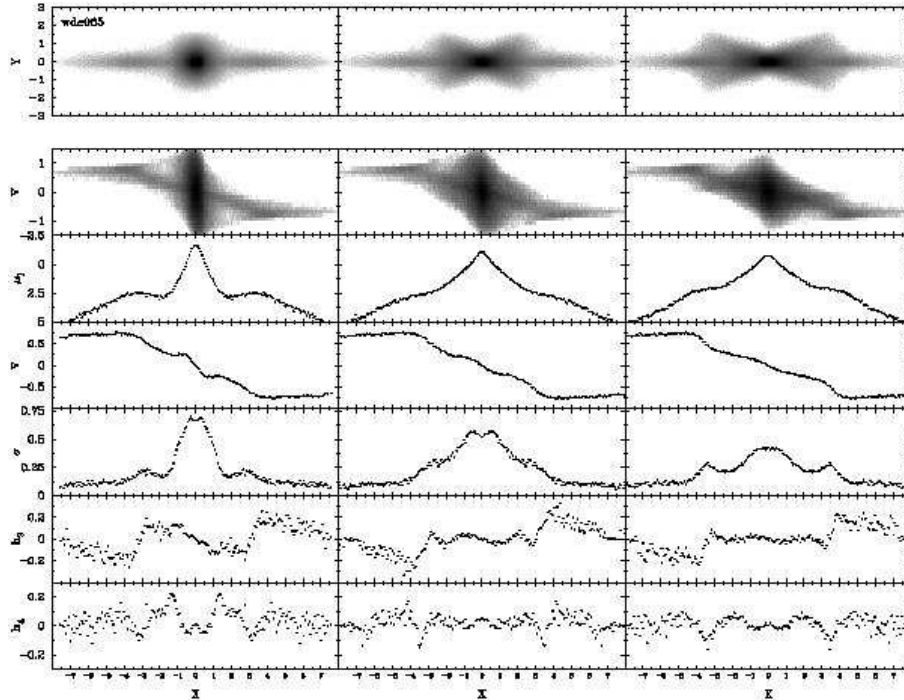


Figure 1. Bar diagnostics as a function of viewing angle for a strong bar. From left to right: simulation seen end-on, at intermediate viewing angle, and side-on. From top to bottom, each panel shows an edge-on view of the simulation, the position-velocity diagram along the major-axis, the major-axis surface brightness profile (μ_I), and the derived Gauss-Hermite coefficients V (mean velocity), σ (velocity dispersion), h_3 (skewness), and h_4 (kurtosis). All grayscales are plotted on a logarithmic scale. Adapted from Bureau & Athanassoula (2004) with permission.

As predicted, galaxies with a B/PS bulge frequently show a double-hump rotation curve with an intermediate dip or plateau, they often display a rather flat central velocity dispersion profile with a secondary peak or plateau, and a significant fraction of the objects have a local central σ minimum ($\geq 40\%$). The h_3 profiles display up to three slope reversals and, most importantly, h_3 is normally correlated with V over the presumed bar length, contrary to expectations from an axisymmetric disk. Figure 2 shows the derived stellar kinematics for 4 objects. The characteristic bar signatures strengthen the case for an intimate relationship between B/PS bulges and bars, even for early-type systems, and they leave little room for competing explanations of the bulges' shape (e.g. Binney & Petrou 1985). We also find that h_3 is anti-correlated with V in the very center of most galaxies ($\geq 60\%$), suggesting that those objects additionally harbor cold and dense (bright) (quasi-)axisymmetric central stellar disks.

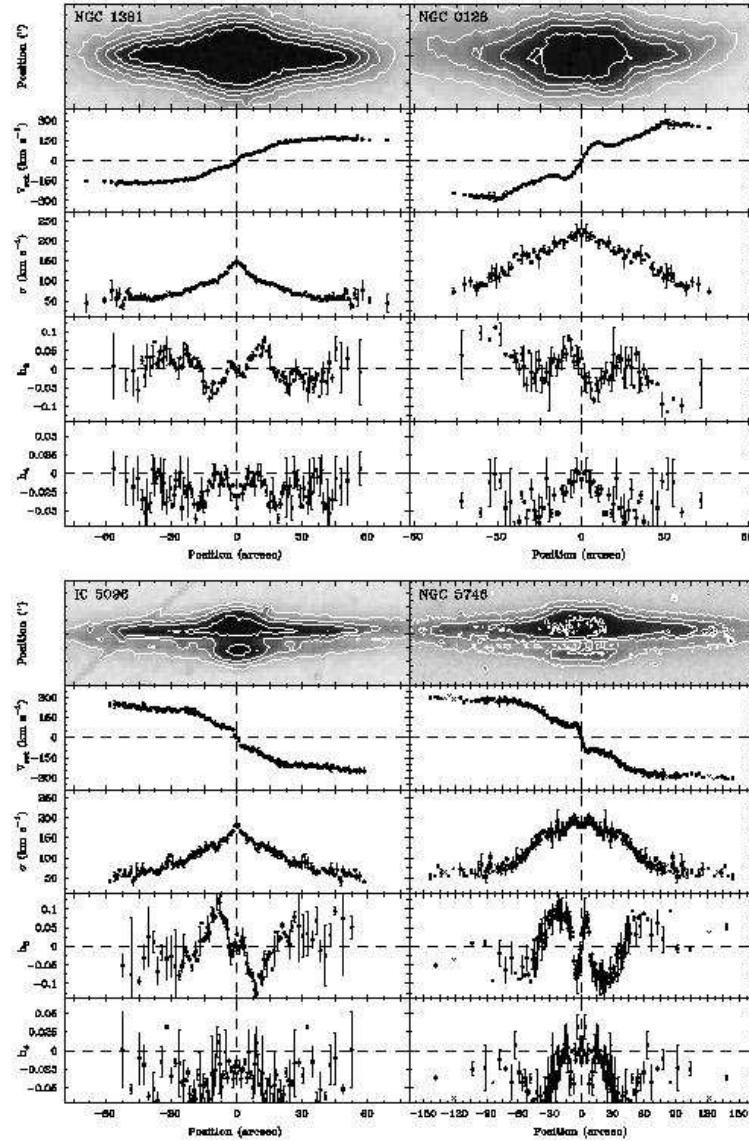


Figure 2. Stellar kinematics of spiral galaxies with a boxy bulge. The galaxies shown are the gas-poor S0 galaxies NGC1381 (top-left) and NGC128 (top-right) and the gas-rich intermediate-type spirals IC5096 (bottom-left) and NGC5746 (bottom-right). From top to bottom, each panel shows an optical image of the galaxy from the Digitized Sky Survey and the registered V , σ , h_3 , and h_4 profiles along the major-axis. The measurements were folded about the center and the errors represent half the difference between the approaching and receding sides. Adapted from Chung & Bureau (2004) with permission.

Those disks may be related to the steep central light profiles observed (§ 4), and they roughly coincide with previously identified star-forming ionized-gas disks (Bureau & Freeman 1999). They thus may well have formed out of gas accumulated by the bar at its center through inflow. As suggested by N-body models, the skewness of the velocity profile (h_3) appears to be a reliable tracer of asymmetries, allowing to discriminate between axisymmetric and barred disks seen in projection. Based on their kinematics, B/PS bulges (and thus a large fraction of all bulges) appear to be made-up mostly of disk material which has acquired a large vertical extent through bar-driven instabilities, although we have not yet probed the potentials of the galaxies out of the disk plane systematically (but see § 5). Our observations are nevertheless consistent with standard bar-driven evolution models, and the formation of B/PS bulges does appear to be dominated by secular evolution processes rather than merging.

4. *K*-Band Imaging of Boxy Bulges

We have also obtained *K*-band images for all the galaxies in our sample. The *K*-band observations penetrate the prominent dust lanes present in many galaxies and offer a much improved view of their structure and morphology, apparently directly constraining the orbital structure of the objects. Indeed, as illustrated in Figure 3 for NGC128, unsharp-masking of those images reveals features entirely analogous to those expected from the orbital families thought to dominate 3D bars (e.g. Patsis, Skokos, & Athanassoula 2002). In particular, the x_1 family “tree” is clearly seen and many galaxies show secondary enhancements along the major-axis (see Skokos, Patsis, & Athanassoula 2002).

Moreover, the key aspect of bar thickening mechanisms to form B/PS bulges is that the disk material is rearranged vertically (as well as radially) by instabilities, rather than new material being added (as expected for accretion scenarios). This process is strongly supported by our observations, as most galaxies show a clear increase of the scaleheight where the B/PS bulge reaches its maximum extent. This is illustrated again in Figure 3 for NGC128, where we fitted the vertical profiles at each (projected) radial position with a generalized Gaussian (equivalent to a Sersic law with $n = \lambda^{-1}$), following Athanassoula & Misiriotis (2002). The shape of the profiles also changes with radius, the profiles being shallower where the peanut shape is maximum. We note that the profiles never approach a deVaucouleurs law ($n = 4$), even in the center, arguing again against violent relaxation and merging. Furthermore, in many galaxies, the steep part of the light profile is much shorter than the vertically-extended component, so that those two definitions of a bulge are clearly inconsistent (as is that of a kinematically hot sub-system, since B/PS bulges are most likely rotationally supported). The steep part of the profiles is thus probably more closely related to the central disks discussed in the previous section.

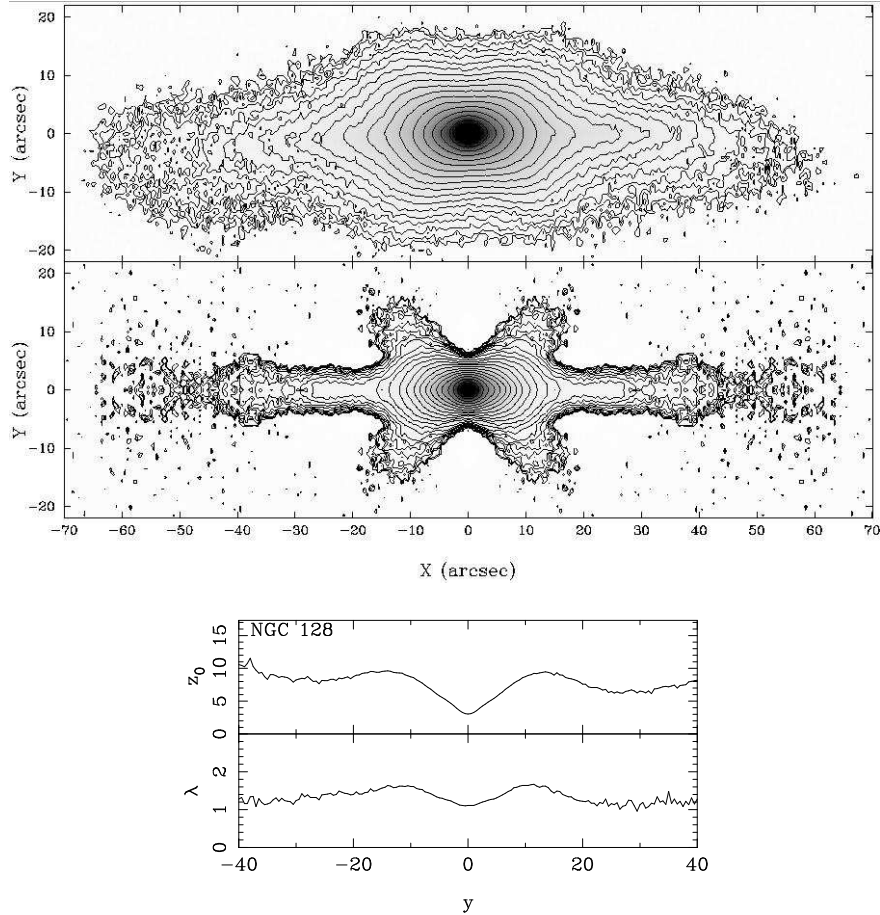


Figure 3. Morphology and structure of spiral galaxies with a boxy bulge. Top: K -band image of the S0 galaxy NGC128, showing the strong peanut-shape of the bulge. The isophotes are separated by $0.5 \text{ mag arcsec}^{-2}$. Middle: Symmetrized unsharp-masked (median-filtered) image of NGC128, revealing the underlying orbital structure. Bottom: Scaleheight (z_0) and shape (λ) of the fitted vertical profiles of NGC128 as a function of projected radius (registered). The radially varying thickening of the disk/bulge material is clearly visible. Adapted from Aronica et al. (2005) and Athanassoula et al. (2005) with permission.

5. SAURON Observations of Boxy Bulges

The SAURON team has conducted a survey of the 2D stellar kinematics, ionized-gas kinematics, and absorption linestrengths of a representative sample of nearby early-type galaxies (e.g. de Zeeuw et al. 2002). The SAURON data on edge-on early-type spirals thus offer a unique opportunity to extend the kinematic tests described above (§ 2) out of the disk plane and to test the predictions of bar-driven evolution scenarios regarding stellar populations.

The best examples are NGC7332 (Falc3n-Barroso et al. 2004) and NGC4526 (Fig. 4; Emsellem et al. 2004; Sarzi et al. 2005; Kuntschner et al. 2005). Both S0 galaxies have a boxy bulge and clearly show the stellar kinematic signatures of a bar. They also possess homogeneous stellar populations (age and metallicity) across the disk and bar/bulge components, except in the central parts, as expected from simple bar-driven evolution models (e.g. Friedli & Benz 1995). NGC4526 also clearly shows a cold central stellar disk embedded in its triaxial bulge, as traced by a strong pinching of the stellar isoveLOCITIES in the center, a wide local central σ minimum, and a strong central $h_3 - V$ anti-correlation (while the rest of the bulge displays an $h_3 - V$ correlation as expected from a thick bar). This central stellar disk coexists with an ionized and molecular gas disk (Young et al. 2005), presumably formed through bar-driven inflow (and ensuing star formation). NGC4526 thus beautifully illustrates and confirms most aspect of bar-driven secular evolution models in spiral galaxies.

6. Conclusions

As secular processes for the evolution of galaxies gain in respect and popularity, developing practical tools to test the various models and gain novel insights into the structure and dynamics of real galaxies becomes increasingly pressing. The stellar kinematic bar diagnostics presented in § 2 allow to identify edge-on bars easily and thus to test the origin of B/PS bulges through bar-driven vertical instabilities. The spectroscopic observations of a large sample of spiral galaxies with a B/PS bulge shown in § 3 vindicate the usefulness of those diagnostics and confirm that B/PS bulges are generally consistent with the presence of a thick bar viewed edge-on, even for the earliest types. They also suggest the presence of rapidly rotating central stellar disks at the center of the bars, which may well have formed through bar-driven inflow and subsequent star formation. Analysis of K -band observations of the same sample reveals the orbital backbone of B/PS bulges (§ 4), in agreement with expectations from periodic orbit calculations of 3D bars. As expected, the scaleheight (and shape) of the material varies rapidly with (projected) radius, and it is largest where the extent of the B/PS bulge is maximum.

The emerging bar-driven evolutionary scenario is beautifully confirmed by synthesis CO observations and SAURON integral-field spectroscopy (§ 5), which further allow to study the distribution of the stellar populations (luminosity-weighted age and metallicity). As the quality of stellar population data is rapidly improving, a parallel improvement of the model predictions (which remain rudimentary) is urgently needed. Interestingly, although clear observational diagnostics of such scenarios are still largely inexistent, our observations do not seem to require nor indicate that bars may be destroyed (and possibly reformed). Specific tests would thus also be appreciated.

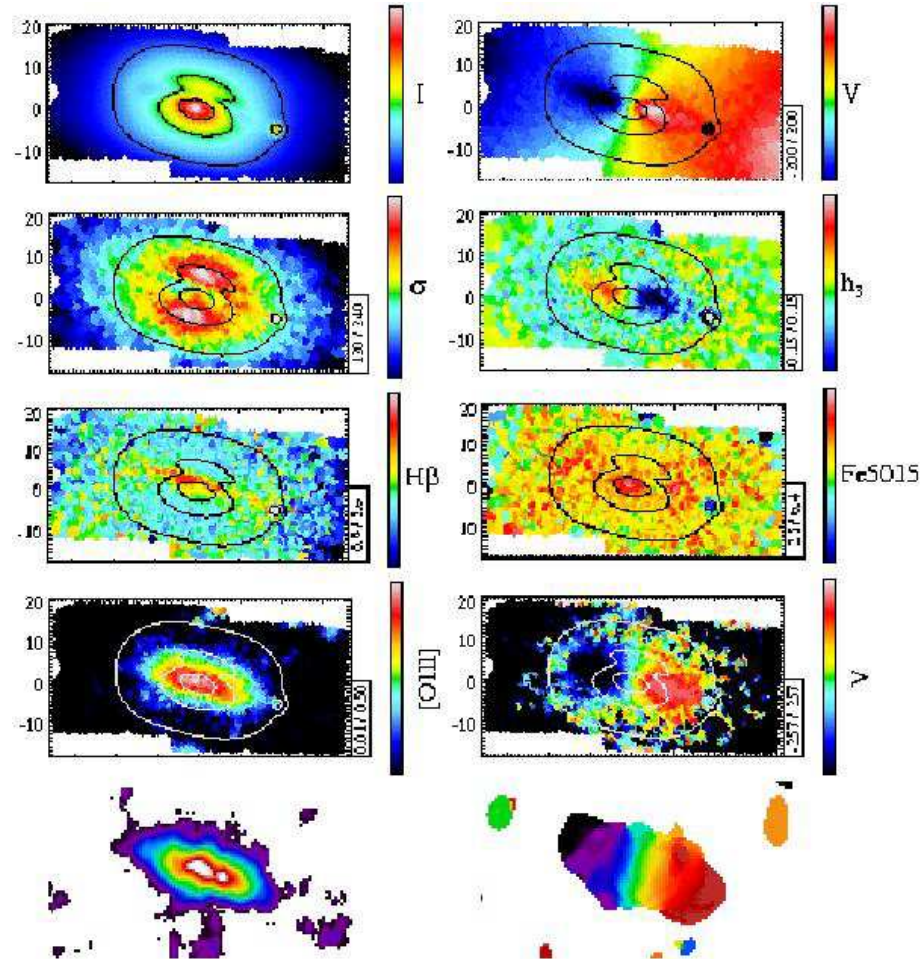


Figure 4. SAURON and BIMA observations of the S0 galaxy NGC4526. From left to right, top to bottom: Reconstructed image, mean stellar velocity V , stellar velocity dispersion σ , asymmetry of the stellar velocity profile h_3 , $H\beta$ line strength (age), Fe5015 line strength (metallicity), [OIII] intensity, ionized-gas velocity, total CO flux, and CO velocity field.

Acknowledgments

M.B. acknowledges support by NASA through Hubble Fellowship grant HST-HF-01136.01 awarded by the Space Telescope Science Institute. The authors wish to thank J.C. Lambert, K.C. Freeman, and E. Emsellem for support and useful discussions, and L. Young and the SAURON Team for data prior to publication. The Digitized Sky Survey was produced at the Space Telescope Science Institute under U.S. Government grant NAG W-2166.

References

- Andredakis, Y. C., Peletier, R. F., & Balcells, M. 1995, *MNRAS*, 275, 874
- Aronica, G., Bureau, M., Athanassoula, E., Dettmar, R.-J., Bosma, A., & Freeman, K. C. 2005, *MNRAS*, in preparation.
- Athanassoula, E. 2003, *MNRAS*, 341, 1179
- Athanassoula, E., Aronica, G., & Bureau, M. 2005, *MNRAS*, in preparation.
- Athanassoula, E., & Bureau, M. 1999, *ApJ*, 522, 699
- Athanassoula, E., & Misiriotis, A. 2002, *MNRAS*, 330, 35
- Binney, J., & Petrou, M. 1985, *MNRAS*, 214, 449
- Bournaud, F., & Combes, F. 2002, *A&A*, 392, 83
- Bureau, M., & Athanassoula, E. 2004, *ApJ*, in press.
- Bureau, M., & Freeman, K. C. 1999, *AJ*, 118, 126
- Combes, F., Debbasch, F., Friedli, D., & Pfenniger, D. 1990, *A&A*, 233, 82
- Combes, F., & Sanders, R. H. 1981, *A&A*, 96, 164
- Chung, A., & Bureau, M. 2004, *AJ*, 127, 3192
- Davies, R. L., Efstathiou, G., Fall, S. M., Illingworth, G., & Schechter, P.L. 1983, *ApJ*, 266, 41
- Emsellem, E., et al. 2004, *MNRAS*, in press.
- Erwin, P., & Sparke, L. S. 2002, *AJ*, 124, 65
- Falcón-Barroso, J., et al. 2004, *MNRAS*, 350, 35
- Friedli, D., & Benz, W. 1993, *A&A*, 268, 65
- Friedli, D., & Benz, W. 1995, *A&A*, 301, 649
- Friedli, D., Wozniak, H., Rieke, M., Martinet, L., & Bratschi, P. 1996, *A&AS*, 118, 461
- Kormendy, J. 1993, in *Galactic Bulges*, eds. H. Dejonghe, & H. J. Habing (Dordrecht: Kluwer), 209
- Kuijken, K., & Merrifield, M. R. 1995, *ApJ*, 443, L13
- Kuntschner, H., et al. 2005, *MNRAS*, submitted.
- Lütticke, R., Dettmar, R.-J., & Pohlen, M. 2000, *A&AS*, 145, 405
- van der Marel, R. P., & Franx, M. 1993, *ApJ*, 407, 525
- Merrifield, M. R., & Kuijken, K. 1999, *A&A*, 443, L47
- Patsis, P. A., Skokos, Ch., & Athanassoula, E. 2002, *MNRAS*, 337, 578
- Pfenniger, D., & Norman, C. 1990, *ApJ*, 363, 391
- Rowley, G. 1988, *ApJ*, 331, 124
- Sarzi, M., et al. 2005, *MNRAS*, in preparation.
- Shen, J., & Sellwood, J. A. 2004, *ApJ*, 604, 614
- Skokos, Ch., Patsis, P. A., & Athanassoula, E. 2002, *MNRAS*, 333, 847
- Young, L. M., et al. 2005, *AJ*, in preparation.
- de Zeeuw, P. T., et al. 2002, *MNRAS*, 329, 513